

Triarylimidazole Redox Catalysts: Electrochemical Analysis and Empirical Correlations

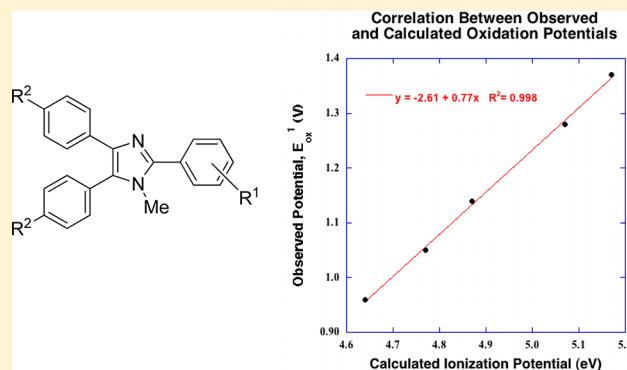
Ni-tao Zhang,[†] Cheng-chu Zeng,^{†,*} Chiu Marco Lam,[‡] Randi K. Gbur,[‡] and R. Daniel Little^{*,‡}

[†]College of Life Science & Bioengineering, Beijing University of Technology, Beijing 100124, China

[‡]Department of Chemistry & Biochemistry, University of California, Santa Barbara, Santa Barbara, California 93106, United States

S Supporting Information

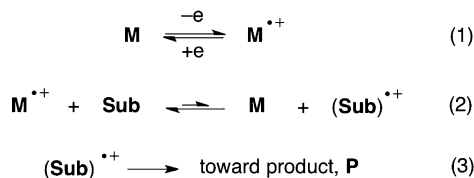
ABSTRACT: A series of triarylimidazoles was synthesized and characterized electrochemically. The synthetic route is general, providing a pathway to 30 redox mediators that exhibit a > 700 mV range of accessible potentials. Most of the triarylimidazoles display three oxidation peaks where the first redox couple is quasi-reversible. The electronic character of the substituents affects the oxidation potential. This is exemplified by a linear correlation between the first oxidation potential and the sum of the Hammett σ^+ substituent constants, as well as with a series of calculated ionization potentials. We close by putting forward a rule of thumb stating that for a given mediator, the upper limit of accessible potentials can be extended by at least 500 mV beyond the largest recorded value. A rationale, the conditions under which the rule is likely to apply, and an example are provided.



INTRODUCTION

A redox mediator can be likened onto a photochemical sensitizer; the latter transfers energy and spin, while a mediator transfers charge.¹ In contrast with direct oxidation and reduction, which take place at an electrode, mediated processes involve homogeneous electron transfer.² Several features render the use of a mediator particularly attractive. Consider for example, the mediated oxidation of a substrate, **Sub**, to form a product, **P** as portrayed in Scheme 1. Now, imagine that the

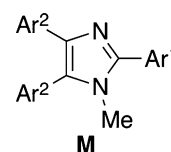
Scheme 1. Avoiding an Impasse and Catalysis



conversion is initiated by a thermodynamically unfavorable electron transfer equilibrium between the mediator, **M**, in its oxidized form, and the substrate (eq 2). This apparent thermodynamic impasse can be overcome provided there is a followup reaction that shifts the equilibrium away from it (eq 3). In this manner, it is possible to use a mediator to achieve the oxidation (reduction) of a substrate at an electrode potential that is less than that required for the direct process. Consequently, the necessary input energy is reduced. This, coupled with the fact that the mediator serves as a catalyst, constitutes two of the attractive features of redox-mediated

processes. In addition, the opportunity to achieve reagent-based selectivity arises, with the mediator serving as the reagent in the role of a homogeneous electron transfer catalyst. As such, one can imagine taking advantage of the structure of the mediator to select between different environments within a substrate in order to achieve site selectivity between two electrophores possessing very similar oxidation/reduction potentials.

Earlier this year we described the synthesis and characterization of five members of a new class of organic redox mediators based on the triarylimidazole scaffold, **M**.³ These substances proved to be stable and easy to synthesize and provided access to a 370 mV window of potentials. They also served as effective mediators for the oxidation of electron-rich benzylic alcohols and ethers, converting each to the corresponding carbonyl compounds in the manner portrayed in Scheme 2.



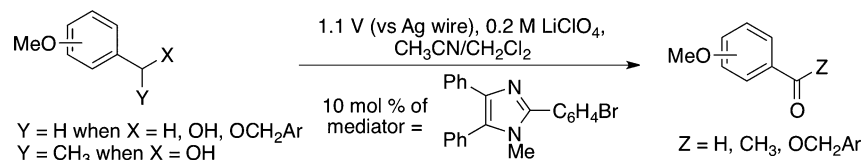
Given these promising results, coupled with the prospect that like the widely used triarylamines,⁴ the triarylimidazoles might find applicability as light emitting devices and/or in lithium ion

Special Issue: Howard Zimmerman Memorial Issue

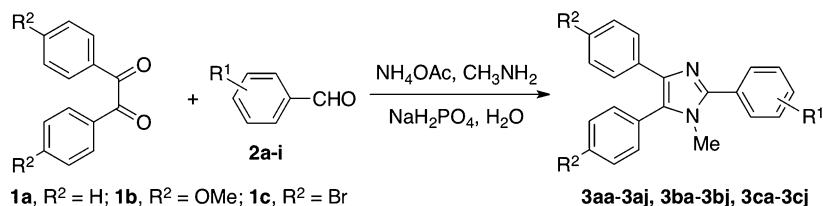
Received: October 23, 2012

Published: November 27, 2012

Scheme 2. Indirect Anodic Oxidation Mediated by 2-(4-Bromophenyl)-1-methyl-4,5-diphenyl-1H-imidazole



Scheme 3. Synthesis of Triarylimidazoles

Table 1. Peak Potential, E_{OX}^1 , of the First Oxidation Peak for Three Series of Triarylimidazoles

Structure	R^1	E_{ox}^1 (V vs Ag/AgCl)		
		3aa-3aj ($R^2 = H$)	3ba-3bj ($R^2 = OMe$)	3ca-3cj ($R^2 = Br$)
3aa, 3ba, 3ca	4-N(Me) ₂	0.77	0.71	0.82
3ab, 3bb, 3cb	3,4-di-OMe	1.14	0.97	1.16
3ac, 3bc, 3cc	4-OMe	1.14	0.96 (0.25) ^a	1.21
3ad, 3bd, 3cd	4-Me	1.22	1.01	1.28
3ae, 3be, 3ce	H	1.23 (0.54) ^a	1.02	1.30
3af, 3bf, 3cf	4-Br	1.28	1.05	1.37 (0.78) ^a
3ag, 3bg, 3cg	4-F	1.29	1.08	1.41
3ah, 3bh, 3ch	3,4-di-F	1.30	1.07	1.37
3ai, 3bi, 3ci	4-CF ₃	1.38	1.10	1.40
3aj, 3bj, 3ej	4-NO ₂	1.37	1.11	1.44

^aThe value in parentheses corresponds to oxidation potential of the correspondingly substituted triarylimine (data from ref 8).

battery research,⁵ we elected to expand the scope of our investigation. Herein we (1) describe the synthesis and electrochemical characterization of a series of 30 triarylimidazoles, (2) demonstrate the generality of the synthetic route, (3) address how the nature of substituents affect the oxidation potential of the mediator, and (4) correlate redox properties with the molecular structures. In addition, we reveal the existence of a linear correlation between the first oxidation potential of the redox catalysts and both Hammett σ^+ substituent constants as well as the calculated ionization potentials.⁶ These correlations allow one to predict the potential for systems yet to be synthesized and will assist in determining which catalyst may be best suited to a particular need.

RESULTS AND DISCUSSION

Synthesis. The synthetic route used to access the mediators is shown in Scheme 3. It follows a known procedure wherein an aqueous solution consisting of a mixture of a benzil (1), an aldehyde (2), methylamine and ammonium acetate in the

presence of a catalytic amount of sodium dihydrogen phosphate, are heated to 150 °C in a thick-walled tube fitted with a screw-on Teflon top.⁷ The reaction proceeds smoothly to afford the desired triarylimidazoles in excellent yields (generally >85%).

Voltammetry. The electrochemical properties of the triarylimidazoles were studied using cyclic voltammetry and the results are summarized in Table 1. Samples were dissolved in a solution of acetonitrile and dichloromethane (4:1 by volume) containing 0.2 M LiClO₄ as the supporting electrolyte. A glassy carbon disk served as the working electrode and a Pt wire the counter electrode. The oxidation potentials, measured at the peak are designated as E_{OX}^1 , and are reported relative to Ag/0.1 M AgCl. With one exception (structure 3ai), all 30 imidazoles exhibit three oxidation peaks and one cathodic peak, the latter being associated with the first of the three peaks (see Supporting Information). Fortunately, the first redox couple is quasi-reversible with the current being slightly smaller during the reduction scan. Thus, the initially formed cation radicals display good stability on the time scale of the CV measurement.

The data in Table 1 is organized into three columns and ten rows. In each column, R^2 is held constant, namely, H for **3aa–3aj**, OMe for **3ba–3bj**, and Br for **3ca–3cj**, while R^1 varies, becoming progressively more electron withdrawing as one reads down a column. For the family **3aa–3aj**, E_{ox}^1 spans from 0.77 for **3aa** ($R^1 = 4\text{-N}(\text{CH}_3)_2$) to 1.37 V for **3aj** ($R^1 = 4\text{-NO}_2$), a range of 600 mV. In the case of redox catalyst **3ae** where R^1 is H, its oxidation potential is 1.23 V. When R^1 is $\text{-N}(\text{Me})_2$, OMe or Me, the potentials shift in accord with the electron donating character of the substituent, from 0.77 V (**3aa**), to 1.14 V (**3ab**), to 1.22 V (**3ad**), respectively. In contrast, the oxidation occurs at more positive potentials when R^1 is electron withdrawing. For example, the oxidation potentials of **3ag** and **3ai** increase to 1.29 and 1.38 V when R^1 is either F or CF_3 , respectively.

Similar trends are observed for the family of redox catalysts **3ba–3bj** ($R^2 = \text{OMe}$) and **3ca–3cj** ($R^2 = \text{Br}$). For the former, the oxidation potentials span 400 mV, changing from 0.71 to 1.11 V, while for **3ca–3cj** the range is 620 mV, spanning from 0.82 to 1.44 V. Once again, we see that the E_{ox}^1 values are affected qualitatively by the electronic character of R^1 , namely, the more electron donating the substituent(s), the easier the substrate is to oxidize.

The E_{ox}^1 values of the redox catalysts are also dependent upon the electronic character of R^2 when values are compared for the same R^1 groups. For example, the oxidation potential of **3aa** ($R^1 = \text{N}(\text{CH}_3)_2$) is 0.77 V, and rises to 0.82 V when an inductively withdrawing Br is introduced, and decreases to 0.71 when OMe is present. Similarly, when $R^1 = \text{H}$, the oxidation potentials changes from 1.23 for **3ae** ($R^2 = \text{H}$), to 1.02 V (**3be**; $R^2 = \text{OMe}$) to 1.30 V (**3ce**, $R^2 = \text{Br}$).

The inductively withdrawing character of Br is clearly evident when one compares the data for the series of redox catalysts **3ae–3af–3ce–3cf**. Each member of the series has one more *p*-Br group than the one following it in the list, and the potentials increase steadily (1.23, 1.28, 1.30 and 1.37 V). It is worth noting that structure **3cf** is the triarylimidazole analog of tris(4-bromophenyl)amine, probably the most frequently used of the triarylamine redox mediators and in this regard, it is of interest to compare their oxidation potentials: for **3cf** the value is 1.37 while for tris(4-bromophenyl)amine, it is 0.78.⁸ Finally, we observe that the potentials for the triarylimidazoles are uniformly larger than those observed for the corresponding triarylamine when the substituents are the same. Compare, for example, the values listed in parentheses in Table 1 for the triphenylimidazole **3ae** ($E_{\text{ox}}^1 = 1.23$) with triphenylamine (0.54), trimethoxyimidazole **3bc** ($E_{\text{ox}}^1 = 0.96$) with its amine counterpart (0.25), and tribromoimidazole **3cf** ($E_{\text{ox}}^1 = 1.37$) with the tribromoamine (0.78).

Computational Analysis and Empirical Relationships.

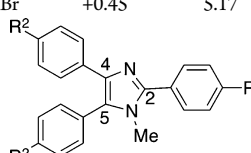
Five of the imidazoles, **3bc**, **3bf**, **3ac**, **3af**, and **3cf**, were examined to determine whether there was an empirical relationship between the first oxidation potential, E_{ox}^1 , and (a) the sum of Hammett σ^+ values for the substituents appended to the three aromatic rings, and/or (b) the calculated ionization potentials (IP).⁹ Should they exist, the correlations would provide a convenient means by which to predict the potential for systems yet to be synthesized and also to assess how effectively these systems respond to changes in their electronic character.^{8,10,11}

IPs were calculated using the B3LYP hybrid functional and a 6-31+G(d) basis set, with acetonitrile as the solvent for both the neutral and cation forms.¹² The cation radical energies

correspond to the geometry-optimized structures. This accords with the philosophy that in contrast with an electronic excitation, the time scale of a voltammetric experiment is significantly longer, thereby giving the ion radical time to relax its geometry to that of an energy minimum. This approach is similar to that previously adopted by Fry and co-workers when they developed empirical relationships for triarylamine.⁸ The calculated IP was then assumed to be the difference in energy between that of the neutral and ion radical forms, each in acetonitrile. Table 2 summarizes the data, and Figures 1 and 2 illustrate the excellent correlations ($R^2 = 0.976$ for $\Sigma\sigma^+$ and 0.998 for IP) as well as the resulting empirical relationships.

Table 2. Summary of Data Used to Correlate Potential with Calculated IP and $\Sigma\sigma^+$

structure	R^1	R^2	$\Sigma\sigma^+$	calculated IP (eV)	E_{ox}^1 (V, vs Ag/AgCl)
3bc	OMe	OMe	-2.34	4.64	0.96
3bf	Br	OMe	-1.41	4.77	1.05
3ac	OMe	H	-0.78	4.87	1.14
3af	Br	H	+0.15	5.07	1.28
3cf	Br	Br	+0.45	5.17	1.37



Interestingly, the slope associated with each correlation is small, namely, 0.144 for $\Sigma\sigma^+$ and 0.770 for IP (note Figure 1). We were surprised to discover that the slopes are also small for the triarylamine and also to note the very similar relationships between the observed potential and calculated IP, it being $-3.190 + 0.789(\text{IP})$ for the triarylamine, and $-2.614 + 0.770(\text{IP})$ for the imidazoles. Thus, neither framework responds dramatically to substituent effects, though each responds in the anticipated manner with the more electron rich systems being easiest to oxidize. Undoubtedly the small slopes are due, at least in part, to the fact that both frameworks must distort to avoid steric interactions, thereby reducing conjugation and therefore, the ability of the substituent to express its character (note Figure 2). The aryl units at C-2 and C-5, positioned closest to the N-methyl group of the imidazole, twist most severely. The torsion angle between the imidazole core and the Ph unit at C-5, for example, is 120° . In addition, interaction between the vicinal aryl groups located at C-4 and C-5 also leads to deviation from planarity. Both distortions are shown clearly in the space-filling rendition of the X-ray structure for **3ac** ($R^1 = \text{OMe}$, $R^2 = \text{H}$), portrayed below.

Concluding Remarks: a Rule of Thumb and a Critique.

The triarylimidazoles are particularly easy to synthesize, leading to a reasonably broad spectrum of structures. Those described allow access to a range of potentials, from 0.71 to 1.44 V, a difference of 730 mV, and nearly double the range that was exhibited by triarylimidazoles prior to this investigation.³ The range is wide enough to allow one to oxidize a host of common functional groups. We suggest that the operational range is even larger based upon the following "rule of thumb", a rule that is intended to serve as a useful guideline.^{4a,13} The rule states that for a mediated electron transfer, the upper limit of accessible potentials can be extended by at least 500 mV, a value that is founded in our work (*vide infra*) and that of others, most

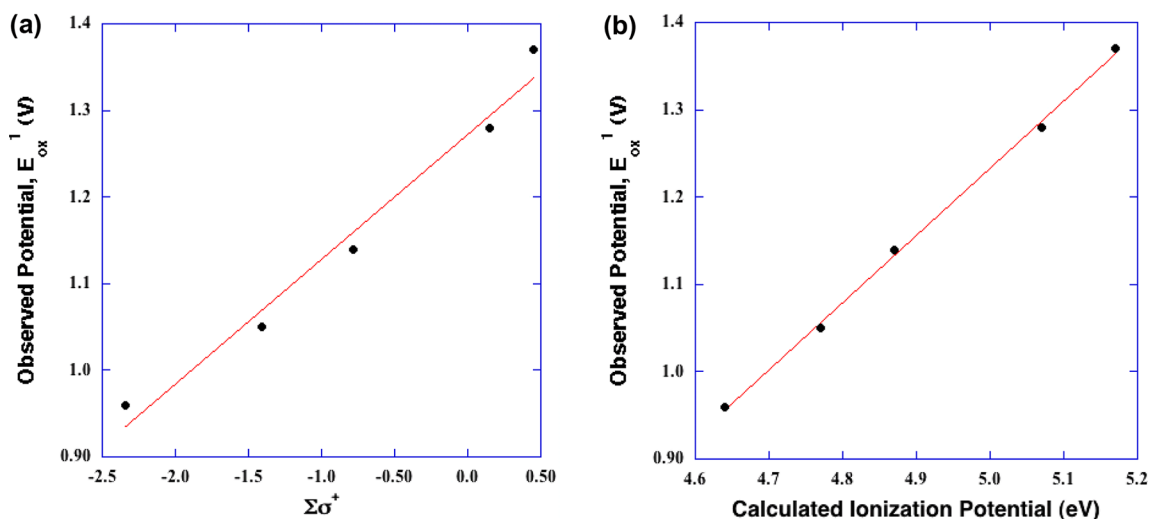


Figure 1. (a) Graph of observed potential vs $\Sigma\sigma^+$ for systems **3bc**, **3bf**, **3ac**, **3af**, and **3cf**. $E_{\text{ox}}^1 = 0.144(\Sigma\sigma^+) + 1.273$ ($R^2 = 0.976$). (b) Graph of observed potential vs calculated IP for systems **3bc**, **3bf**, **3ac**, **3af**, and **3cf**. $E_{\text{ox}}^1 = 0.770(\text{IP}) - 2.614$ ($R^2 = 0.998$).

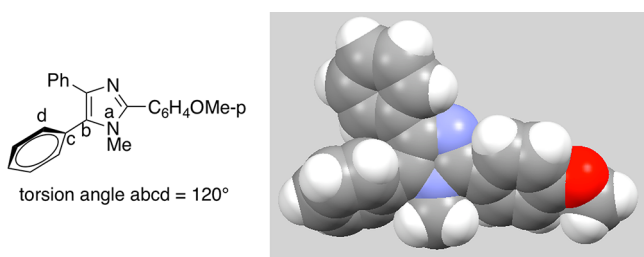
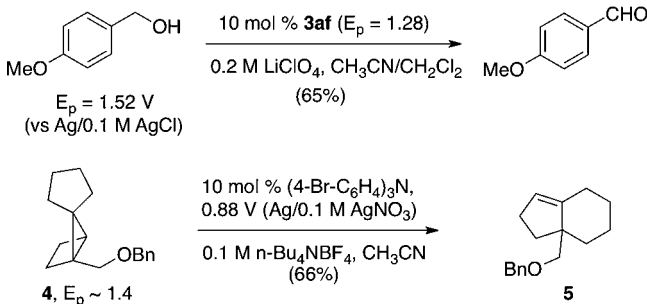


Figure 2. Twisting of the aryl groups out of planarity reduces interaction with substituents.

notably the late Eberhard Steckhan.^{13,14} The implication is that one can use the mediator to oxidize (reduce) a substrate whose oxidation (reduction) potential exceeds that of the mediator by 500 mV, perhaps more, depending upon the equilibrium constant for the electron transfer and the rate of the followup reaction that drains the unfavorable equilibrium (note Scheme 1).¹³

The examples shown in Scheme 4 illustrate the rule of thumb in action. In the first instance,³ the mediated oxidation of *p*-

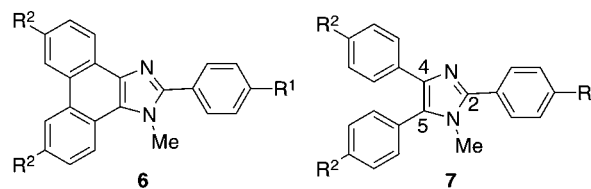
Scheme 4. Two Examples of the “Rule of Thumb” in Action



methoxybenzyl alcohol was carried out at the potential of the mediator. Nevertheless, it occurs smoothly despite the fact that the triarylimidazole **3af** is 260 mV easier to oxidize than the substrate. The second example, stemming from our previous exploration of the use of triarylamine mediators in synthesis,^{14b} exemplifies the rearrangement of the strained hydrocarbon **4**

using tris(4-bromophenyl)amine as the mediator, a substance that is ~520 mV easier to oxidize than the substrate. Yet, when the operating potential is set at that of the mediator, the rearrangement occurs smoothly to deliver **5** in a 66% isolated yield.

While the range of accessible potentials is good, the significant distortion from planarity presents a problem, one that undoubtedly limits the effectiveness of substituents to influence potential. One way to obviate this problem would be to link the ortho carbons of the aromatics positioned at C-4 and C-5 to generate the fused framework **6**.¹⁵ Whether the anticipated improvement in behavior/properties will be manifested remains to be seen.



EXPERIMENTAL SECTION

General Information. All solvents were of commercial quality and were dried and purified by conventional methods. The ¹H NMR and ¹³C NMR spectra were obtained using either a 300 or 400 MHz spectrometer in solvent (CDCl₃) with TMS as internal reference. Data for structures **3ac**, **3af**, **3bc**, **3bf**, **3cf** have been reported previously.³ High resolution mass spectra were obtained using a time-of-flight (TOF) mass spectrometer fitted with an electron ionization (EI) source.

General Procedure for the Synthesis of Triarylimidazoles. A mixture of the benzil of choice (5 mmol), methylamine (5 mmol; or another amine of interest), aldehyde (5 mmol), ammonium acetate (5 mmol) and NaH₂PO₄ (1.5 mmol) was added to a thick-walled test tube with a screw-on Teflon top. The reaction mixture was heated to 150 °C and maintained at the temperature for 2–5 h; the reaction mixture was stirred throughout. Then the reaction mixture was cooled to room temperature. Acetone was added to dissolve the mixture and the undissolved residue was removed by filtration. After evaporation of the solvent under reduced pressure, the resulting solid residue was recrystallized from acetone–water to obtain pure products **3**.

***N,N*-Dimethyl-4-(1-methyl-4,5-diphenyl-1H-imidazol-2-yl)-aniline (3aa):**¹⁶ 325.2 mg, 92% yield; brown powder, mp: 227–229 °C; ¹H NMR (400 MHz, CDCl₃): δ 3.02 (s, 6H), 3.49 (s, 3H), 6.80 (d, *J* = 8.8 Hz, 2H), 7.11–7.15 (m, 1H), 7.19–7.22 (m, 2H), 7.40–7.48 (m, 5H), 7.56 (d, *J* = 7.2 Hz, 2H), 7.63 (d, *J* = 8.8 Hz, 2H).

2-(3,4-Dimethoxyphenyl)-1-methyl-4,5-diphenyl-1H-imidazole (3ab): 314.9 mg, 85% yield; white needles, mp: 197–198 °C; IR (KBr): ν 3436, 2955, 1602, 1586, 1528, 1322 cm⁻¹; ¹H NMR (400 MHz, CDCl₃): δ 3.52 (s, 3H), 3.96 (s, 3H), 4.00 (s, 3H), 6.98 (d, *J* = 8.4 Hz, 1H), 7.16 (t, *J* = 6.8 Hz, 1H), 7.21–7.25 (m, 3H), 7.37 (s, 1H), 7.42–7.58 (m, 7H); ¹³C NMR (100 MHz, CDCl₃): δ 33.2, 55.9, 56.0, 110.8, 111.5, 121.5, 123.7, 126.3, 127.0, 128.1, 128.5, 129.0, 130.3, 130.9, 131.3, 134.6, 137.4, 147.9, 149.0, 149.6. HRESI-MS (*m/z*) calcd. for C₂₄H₂₃N₂O₂ (M + H) 371.1760, found 371.1749.

1-Methyl-4,5-diphenyl-2-(*p*-tolyl)-1H-imidazole (3ad):¹⁷ 292.0 mg, 90% yield; white needles, mp: 211–212 °C; ¹H NMR (400 MHz, CDCl₃): δ 2.42 (s, 3H), 3.50 (s, 3H), 7.12–7.16 (m, 1H), 7.19–7.23 (m, 2H), 7.30 (d, *J* = 8.0 Hz, 2H), 7.40–7.48 (m, 5H), 7.54–7.56 (m, 2H), 7.64 (d, *J* = 8.0 Hz, 2H).

1-Methyl-2,4,5-triphenyl-1H-imidazole (3ae):¹³ 276.2 mg, 89% yield; white needle, mp: 143–145 °C; ¹H NMR (400 MHz, CDCl₃): δ 3.51 (s, 3H), 7.15–7.17 (m, 1H), 7.20–7.24 (m, 2H), 7.40–7.52 (m, 8H), 7.54–7.57 (m, 2H), 7.75–7.77 (m, 2H).

2-(4-Fluorophenyl)-1-methyl-4,5-diphenyl-1H-imidazole (3ag): 279.1 mg, 85% yield; yellow powder, mp: 158–160 °C; IR (KBr): ν 3440, 2919, 2850, 1603, 1528, 1467, 1225 cm⁻¹; ¹H NMR (400 MHz, CDCl₃): δ 3.49 (s, 3H), 7.13–7.23 (m, 5H), 7.41 (d, *J* = 7.6 Hz, 2H), 7.45–7.54 (m, 5H), 7.71–7.75 (m, 2H); ¹³C NMR (100 MHz, CDCl₃): δ 33.1, 115.6 (d, *J*_{C-F} = 22.0 Hz), 126.4, 126.9, 127.1 (d, *J*_{C-F} = 3.0 Hz), 128.1, 128.7, 129.1, 130.5, 130.8, 130.9 (d, *J*_{C-F} = 9.0 Hz), 131.1, 134.5, 137.7, 146.9, 163.0 (d, *J*_{C-F} = 247.0 Hz). HRESI-MS (*m/z*) calcd. for C₂₂H₁₇N₂F (M) 328.1376, found 328.1359, calcd. for C₂₂H₁₆N₂F (M - H) 327.1298, found 327.1302.

2-(3,4-Difluorophenyl)-1-methyl-4,5-diphenyl-1H-imidazole (3ah): 287.5 mg, 83% yield; white powder, mp: 130–131 °C; IR (KBr): ν 3434, 2918, 2850, 1603, 1535, 1501, 1484, 1225 cm⁻¹; ¹H NMR (400 MHz, CDCl₃): δ 3.51 (s, 3H), 7.15–7.24 (m, 3H), 7.28–7.33 (m, 1H), 7.39–7.41 (m, 2H), 7.48–7.53 (m, 6H), 7.60–7.64 (m, 1H); ¹³C NMR (100 MHz, CDCl₃): δ 33.1, 117.6 (d, *J*_{C-F} = 17.0 Hz), 118.3 (d, *J*_{C-F} = 18.0 Hz), 125.1, 125.2 (dd, *J*_{C-F} = 6.0, 4.0 Hz), 126.5, 126.9, 127.9–128.0 (m), 128.2, 128.8, 129.1, 130.8, 130.9, 134.3, 138.0, 145.7, 150.3 (dd, *J*_{C-F} = 250.0, 15.0 Hz), 150.7 (dd, *J*_{C-F} = 252.0, 16.0 Hz). HRESI-MS (*m/z*) calcd. for C₂₂H₁₅N₂F₂ (M) 346.1282, found 346.1273, calcd. for C₂₂H₁₅N₂F₂ (M - H) 345.1203, found 345.1213.

1-Methyl-4,5-diphenyl-2-(4-(trifluoromethyl)phenyl)-1H-imidazole (3ai): 321.6 mg, 85% yield; white powder, mp: 147–148 °C; IR (KBr): ν 3432, 2923, 1616, 1324, 1160 cm⁻¹; ¹H NMR (400 MHz, CDCl₃): δ 3.55 (s, 3H), 7.15–7.25 (m, 3H), 7.41–7.43 (m, 2H), 7.46–7.55 (m, 5H), 7.76 (d, *J* = 8.0 Hz, 2H), 7.92 (d, *J* = 8.0 Hz, 2H); ¹³C NMR (100 MHz, CDCl₃): δ 33.3, 125.6 (q, *J*_{C-F} = 4.0 Hz), 126.6, 126.9, 128.2, 128.8, 129.1, 129.2, 130.7, 130.8, 130.9, 131.2, 134.3, 134.4, 138.3, 146.3; HRESI-MS (*m/z*) calcd. for C₂₃H₁₇N₂F₃ (M) 378.1344, found 378.1330, calcd. for C₂₃H₁₆N₂F₃ (M - H) 377.1266, found 377.1274.

1-Methyl-2-(4-nitrophenyl)-4,5-diphenyl-1H-imidazole (3aj):¹⁸ 316.3 mg, 89% yield; golden-colored powder, mp: 199–200 °C; ¹H NMR (400 MHz, CDCl₃): δ 3.59 (s, 3H), 7.18–7.24 (m, 3H), 7.40–7.43 (m, 2H), 7.49–7.54 (m, 5H), 7.99 (d, *J* = 8.8 Hz, 2H), 8.37 (d, *J* = 8.8 Hz, 2H).

4-(4,5-Bis(4-methoxyphenyl)-1-methyl-1H-imidazol-2-yl)-*N,N*-dimethylaniline (3ba): 372.2 mg, 90% yield; yellow powder, mp: 153–154 °C; IR (KBr): ν 3436, 2920, 1612, 1563, 1518, 1247 cm⁻¹; ¹H NMR (400 MHz, CDCl₃): δ 3.02 (s, 6H), 3.46 (s, 3H), 3.76 (s, 3H), 3.87 (s, 3H), 6.76 (d, *J* = 8.8 Hz, 2H), 6.80 (d, *J* = 8.8 Hz, 2H), 6.99 (d, *J* = 8.8 Hz, 2H), 7.31 (d, *J* = 8.4 Hz, 2H), 7.50 (d, *J* = 8.4 Hz, 2H), 7.60 (d, *J* = 8.4 Hz, 2H); ¹³C NMR (100 MHz, CDCl₃): δ 33.0, 40.4, 55.1, 55.3, 112.0, 113.4, 114.4, 118.9, 123.8, 127.9, 128.0, 128.7, 129.9, 132.2, 136.9, 148.2, 150.5, 158.0, 159.5. HRESI-MS (*m/z*) calcd. for C₂₆H₂₈N₃O₂ (M + H) 414.2182, found 414.2177.

2-(3,4-Dimethoxyphenyl)-4,5-bis(4-methoxyphenyl)-1-methyl-1H-imidazole (3bb): 347.0 mg, 86% yield; yellow powder, mp: 125–126 °C; IR (KBr): ν 3436, 2932, 1611, 1519, 1494 cm⁻¹; ¹H NMR (400 MHz, CDCl₃): δ 3.47 (s, 3H), 3.77 (s, 3H), 3.88 (s, 3H), 3.94 (s, 3H), 3.98 (s, 3H), 6.77 (d, *J* = 8.8 Hz, 2H), 6.95–6.97 (m, 1H), 7.00 (d, *J* = 8.8 Hz, 2H), 7.19–7.21 (m, 1H), 7.31–7.33 (m, 3H), 7.49 (d, *J* = 8.8 Hz, 2H); ¹³C NMR (100 MHz, CDCl₃): δ 33.0, 55.1, 55.3, 56.0, 56.1, 110.9, 112.6, 113.5, 114.5, 121.4, 123.5, 123.9, 127.6, 128.0, 129.1, 132.2, 137.1, 147.4, 149.1, 149.5, 158.2, 159.7. HRESI-MS (*m/z*) calcd. for C₂₆H₂₇N₂O₄ (M + H) 431.1971, found 431.1962.

4,5-Bis(4-methoxyphenyl)-1-methyl-2-(*p*-tolyl)-1H-imidazole (3bd): 342.2 mg, 89% yield; yellow needles, mp: 129–131 °C; IR (KBr): ν 3435, 2919, 1614, 1517, 1495, 1247 cm⁻¹; ¹H NMR (400 MHz, CDCl₃): δ 2.42 (s, 3H), 3.46 (s, 3H), 3.76 (s, 3H), 3.88 (s, 3H), 6.77 (d, *J* = 8.8 Hz, 2H), 7.00 (d, *J* = 8.4 Hz, 2H), 7.29 (d, *J* = 8.0 Hz, 2H), 7.32 (d, *J* = 8.8 Hz, 2H), 7.49 (d, *J* = 8.8 Hz, 2H), 7.62 (d, *J* = 8.0 Hz, 2H); ¹³C NMR (100 MHz, CDCl₃): δ 21.4, 33.0, 55.2, 55.3, 113.5, 114.5, 123.5, 127.6, 128.0, 128.2, 128.9, 129.1, 129.2, 132.2, 137.2, 138.5, 147.5, 158.1, 159.7. HRESI-MS (*m/z*) calcd. for C₂₅H₂₄N₂O₂ (M) 384.1838, found 384.1850.

4,5-Bis(4-methoxyphenyl)-1-methyl-2-phenyl-1H-imidazole (3be): 326.0 mg, 88% yield; white needles, mp: 158–161 °C; ¹H NMR (300 MHz, CDCl₃): δ 3.48 (s, 3H), 3.76 (s, 3H), 3.87 (s, 3H), 6.77 (d, *J* = 9.0 Hz, 2H), 7.00 (d, *J* = 8.7 Hz, 2H), 7.31 (d, *J* = 8.7 Hz, 2H), 7.40–7.51 (m, 5H), 7.73–7.75 (m, 2H).

2-(4-Fluorophenyl)-4,5-bis(4-methoxyphenyl)-1-methyl-1H-imidazole (3bg): 314.6 mg, 81% yield; yellow powder, mp: 148–150 °C; IR (KBr): ν 3435, 2938, 2837, 1612, 1519, 1495, 1248 cm⁻¹; ¹H NMR (400 MHz, CDCl₃): δ 3.46 (s, 3H), 3.77 (s, 3H), 3.88 (s, 3H), 6.77 (d, *J* = 8.8 Hz, 2H), 7.00 (d, *J* = 8.8 Hz, 2H), 7.18 (t, *J* = 8.8 Hz, 2H), 7.31 (d, *J* = 8.8 Hz, 2H), 7.48 (d, *J* = 8.8 Hz, 2H), 7.72 (dd, *J* = 8.4, 5.2 Hz, 2H); ¹³C NMR (100 MHz, CDCl₃): δ 33.0, 55.2, 55.3, 113.6, 114.5, 115.6 (d, *J*_{C-F} = 22.0 Hz), 123.3, 127.2, 127.4, 128.0, 129.3, 130.9 (d, *J*_{C-F} = 8.0 Hz), 132.2, 137.3, 146.4, 158.2, 159.8, 163.0 (d, *J*_{C-F} = 248.0 Hz). HRESI-MS (*m/z*) calcd. for C₂₄H₂₁N₂O₂F (M) 388.1587, found 388.1585.

2-(3,4-Difluorophenyl)-4,5-bis(4-methoxyphenyl)-1-methyl-1H-imidazole (3bh): 357.6 mg, 88% yield; yellow powder, mp: 135–137 °C; IR (KBr): ν 3436, 2928, 2838, 1609, 1519, 1495, 1247 cm⁻¹; ¹H NMR (400 MHz, CDCl₃): δ 3.48 (s, 3H), 3.77 (s, 3H), 3.88 (s, 3H), 6.77 (d, *J* = 8.4 Hz, 2H), 7.01 (d, *J* = 8.8 Hz, 2H), 7.24–7.32 (m, 3H), 7.45–7.46 (m, 3H), 7.57–7.62 (m, 1H); ¹³C NMR (100 MHz, CDCl₃): δ 33.0, 55.2, 55.3, 113.6, 114.6, 117.5 (d, *J*_{C-F} = 18.0 Hz), 118.1 (d, *J*_{C-F} = 19.0 Hz), 123.0, 125.1 (dd, *J*_{C-F} = 3.0, 3.0 Hz), 127.2, 128.0, 128.0–128.2 (m), 129.8, 132.1, 137.7, 145.2, 150.3 (d, *J*_{C-F} = 234.0 Hz), 150.6 (dd, *J*_{C-F} = 234.0, 10.0 Hz), 158.3, 159.9; HRESI-MS (*m/z*) calcd. for C₂₄H₂₁N₂O₂F₂ (M + H) 407.1571, found 407.1563.

4,5-Bis(4-methoxyphenyl)-1-methyl-2-(4-(trifluoromethyl)phenyl)-1H-imidazole (3bi): 368.3 mg, 84% yield; yellow powder, mp: 141–144 °C; IR (KBr): ν 3436, 2949, 2837, 1616, 1517, 1328 cm⁻¹; ¹H NMR (400 MHz, CDCl₃): δ 3.52 (s, 3H), 3.77 (s, 3H), 3.88 (s, 3H), 6.78 (d, *J* = 8.8 Hz, 2H), 7.01 (d, *J* = 8.4 Hz, 2H), 7.32 (d, *J* = 8.4 Hz, 2H), 7.48 (d, *J* = 8.8 Hz, 2H), 7.74 (d, *J* = 8.4 Hz, 2H), 7.89 (d, *J* = 8.0 Hz, 2H); ¹³C NMR (100 MHz, CDCl₃): δ 33.2, 55.2, 55.3, 113.6, 114.3, 114.6, 122.8, 125.5 (q, *J*_{C-F} = 4.0 Hz), 127.0, 128.1, 129.2, 130.2, 132.1, 132.4, 134.3, 137.9, 145.8, 158.4, 159.9; HRESI-MS (*m/z*) calcd. for C₂₅H₂₂N₂O₂F₃ (M + H) 439.1633, found 439.1621.

4,5-Bis(4-methoxyphenyl)-1-methyl-2-(4-nitrophenyl)-1H-imidazole (3bj):¹⁹ 361.4 mg, 87% yield; orange powder, mp: 123–125 °C; ¹H NMR (400 MHz, CDCl₃): δ 3.57 (s, 3H), 3.78 (s, 3H), 3.89 (s, 3H), 6.79 (d, *J* = 8.8 Hz, 2H), 7.02 (d, *J* = 8.8 Hz, 2H), 7.32 (d, *J* = 8.8 Hz, 2H), 7.48 (d, *J* = 8.0 Hz, 2H), 7.97 (d, *J* = 8.8 Hz, 2H), 8.35 (d, *J* = 8.8 Hz, 2H).

4-(4,5-Bis(4-bromophenyl)-1-methyl-1H-imidazol-2-yl)-*N,N*-dimethylaniline (3ca): 460.1 mg, 90% yield; yellow powder, mp: 212–214 °C; IR (KBr): ν 3434, 2920, 2838, 1612, 1543, 1487, 1443 cm⁻¹; ¹H NMR (400 MHz, CDCl₃): δ 3.03 (s, 6H), 3.48 (s, 3H), 6.80 (d, *J* = 8.8 Hz, 2H), 7.26 (d, *J* = 8.4 Hz, 2H), 7.34 (d, *J* = 8.4 Hz, 2H), 7.40 (d, *J* = 8.4 Hz, 2H), 7.58 (d, *J* = 8.4 Hz, 2H), 7.60 (d, *J* = 8.0 Hz,

2H); ^{13}C NMR (100 MHz, CDCl_3): δ 33.3, 40.3, 112.0, 118.0, 120.2, 122.9, 128.6, 128.8, 129.9, 130.2, 131.2, 132.3, 132.4, 133.7, 149.3, 150.7; HREI-MS (m/z) calcd. for $\text{C}_{24}\text{H}_{21}\text{N}_3\text{Br}_2$ (M) 509.0102, found 509.0089, calcd. for $\text{C}_{24}\text{H}_{20}\text{N}_3\text{Br}_2$ (M - H) 508.0024, found 508.0006.

4,5-Bis(4-bromophenyl)-2-(3,4-dimethoxyphenyl)-1-methyl-1H-imidazole (3cb): 449.0 mg, 85% yield; white powder, mp: 176–178 °C; IR (KBr): ν 3466, 2921, 1631, 1531, 1488, 1224 cm^{-1} ; ^1H NMR (400 MHz, CDCl_3): δ 3.50 (s, 3H), 3.95 (s, 3H), 3.98 (s, 3H), 6.97 (d, $J = 8.4$ Hz, 1H), 7.19–7.21 (m, 1H), 7.27 (d, $J = 8.0$ Hz, 2H), 7.31 (s, 1H), 7.35 (d, $J = 8.4$ Hz, 2H), 7.40 (d, $J = 8.4$ Hz, 2H), 7.62 (d, $J = 8.4$ Hz, 2H); ^{13}C NMR (100 MHz, CDCl_3): δ 33.3, 56.0, 56.1, 110.9, 112.5, 120.4, 121.5, 123.1, 128.6, 129.2, 129.8, 131.3, 132.3, 132.5, 133.3, 136.8, 148.4, 149.1, 149.8. HRESI-MS (m/z) calcd. for $\text{C}_{24}\text{H}_{21}\text{N}_2\text{O}_2\text{Br}_2$ (M + H) 526.9970, found 526.9954.

4,5-Bis(4-bromophenyl)-2-(4-methoxyphenyl)-1-methyl-1H-imidazole (3cc): 413.5 mg, 83% yield; white powder, mp: 145–147 °C; IR (KBr): ν 3434, 2953, 2924, 1612, 1577, 1531, 1479, 1402, 838 cm^{-1} ; ^1H NMR (400 MHz, CDCl_3): δ 3.47 (s, 3H), 3.87 (s, 3H), 7.02 (d, $J = 8.8$ Hz, 2H), 7.26 (d, $J = 8.4$ Hz, 2H), 7.34 (d, $J = 8.4$ Hz, 2H), 7.39 (d, $J = 8.8$ Hz, 2H), 7.62 (d, $J = 8.4$ Hz, 2H), 7.64 (d, $J = 8.8$ Hz, 2H); ^{13}C NMR (100 MHz, CDCl_3): δ 33.2, 55.4, 114.1, 120.4, 123.0, 123.1, 128.5, 129.1, 129.9, 130.4, 131.3, 132.3, 132.5, 133.4, 136.8, 148.4, 160.2. HREI-MS (m/z) calcd. for $\text{C}_{23}\text{H}_{18}\text{N}_2\text{OBr}_2$ (M) 495.9786, found 495.9786.

4,5-Bis(4-bromophenyl)-1-methyl-2-(p-tolyl)-1H-imidazole (3cd): 400.2 mg, 83% yield; white powder, mp: 189–190 °C; IR (KBr): ν 3433, 2919, 1638, 1478, 1391, 833 cm^{-1} ; ^1H NMR (400 MHz, CDCl_3): δ 2.42 (s, 3H), 3.49 (s, 3H), 7.27 (d, $J = 8.4$ Hz, 2H), 7.30 (d, $J = 8.0$ Hz, 2H), 7.35 (d, $J = 8.8$ Hz, 2H), 7.40 (d, $J = 8.8$ Hz, 2H), 7.59–7.63 (m, 4H); ^{13}C NMR (100 MHz, CDCl_3): δ 21.4, 33.2, 120.4, 123.1, 127.6, 128.6, 128.9, 129.2, 129.4, 129.9, 131.3, 132.3, 132.5, 133.4, 137.0, 139.0, 148.6. HREI-MS (m/z) calcd. for $\text{C}_{23}\text{H}_{18}\text{N}_2\text{Br}_2$ (M) 479.9837, found 479.9831.

4,5-Bis(4-bromophenyl)-1-methyl-2-phenyl-1H-imidazole (3ce): 412.0 mg, 88% yield; white powder, mp: 201–203 °C; IR (KBr): ν 3435, 3061, 2920, 1494, 1474, 837 cm^{-1} ; ^1H NMR (300 MHz, CDCl_3): δ 3.50 (s, 3H), 7.27 (d, $J = 8.4$ Hz, 2H), 7.35 (d, $J = 8.7$ Hz, 2H), 7.40 (d, $J = 8.7$ Hz, 2H), 7.45–7.53 (m, 3H), 7.63 (d, $J = 8.4$ Hz, 2H), 7.70–7.73 (m, 2H); ^{13}C NMR (100 MHz, CDCl_3): δ 33.2, 120.5, 123.2, 128.6, 128.7, 129.0, 129.4, 129.8, 130.5, 131.3, 132.3, 132.5, 133.3, 137.1, 148.5. HRESI-MS (m/z) calcd. for $\text{C}_{22}\text{H}_{16}\text{N}_2\text{Br}_2$ (M) 465.9680, found 465.9689.

4,5-Bis(4-bromophenyl)-2-(4-fluorophenyl)-1-methyl-1H-imidazole (3cg): 393.8 mg, 81% yield; white powder, mp: 172–174 °C; IR (KBr): ν 3450, 2919, 1639, 1479, 1447, 833 cm^{-1} ; ^1H NMR (400 MHz, CDCl_3): δ 3.48 (s, 3H), 7.20 (d, $J = 8.4$ Hz, 1H), 7.22 (d, $J = 8.8$ Hz, 1H), 7.26 (d, $J = 8.4$ Hz, 2H), 7.35 (d, $J = 8.8$ Hz, 2H), 7.39 (d, $J = 8.8$ Hz, 2H), 7.63 (d, $J = 8.4$ Hz, 2H), 7.70 (d, $J = 8.4$ Hz, 1H), 7.72 (d, $J = 8.4$ Hz, 1H); ^{13}C NMR (100 MHz, CDCl_3): δ 33.2, 115.8 (d, $J_{\text{C-F}} = 21.0$ Hz), 120.5, 123.3, 126.8, 128.5, 129.4, 129.7, 130.9 (d, $J_{\text{C-F}} = 4.0$ Hz), 131.3, 132.3, 132.5, 133.2, 137.1, 147.5, 163.2 (d, $J_{\text{C-F}} = 248.0$ Hz). HREI-MS (m/z) calcd. for $\text{C}_{22}\text{H}_{15}\text{N}_2\text{Br}_2\text{F}$ (M) 483.9586, found 483.9580, calcd. for $\text{C}_{22}\text{H}_{14}\text{N}_2\text{Br}_2\text{F}$ (M - H) 482.9508, found 482.9509.

4,5-Bis(4-bromophenyl)-2-(3,4-difluorophenyl)-1-methyl-1H-imidazole (3ch): 438.6 mg, 87% yield; white powder, mp: 144–146 °C; IR (KBr): ν 3449, 1604, 1568, 1533, 1484, 1321, 835 cm^{-1} ; ^1H NMR (400 MHz, CDCl_3): δ 3.50 (s, 3H), 7.24–7.33 (m, 3H), 7.34–7.39 (m, 4H), 7.45–7.47 (m, 1H), 7.56–7.60 (m, 1H), 7.62–7.64 (m, 2H); ^{13}C NMR (100 MHz, CDCl_3): δ 33.2, 117.7 (dd, $J_{\text{C-F}} = 14.0, 5.0$ Hz), 118.3 (d, $J_{\text{C-F}} = 18$ Hz, 2.0 Hz), 120.7, 123.4, 125.2 (t, $J_{\text{C-F}} = 5.0$ Hz), 127.0–127.6 (m), 128.5, 129.4, 129.8, 131.4, 132.3, 132.6, 133.0, 137.3, 146.3, 150.3 (dd, $J_{\text{C-F}} = 250.0$ Hz, 15.0 Hz), 150.9 (dd, $J_{\text{C-F}} = 251.0$ Hz, 14.0 Hz). HRESI-MS (m/z) calcd. for $\text{C}_{22}\text{H}_{14}\text{N}_2\text{Br}_2\text{F}_2$ (M) 501.9492, found 501.9485.

4,5-Bis(4-bromophenyl)-1-methyl-2-[4-(trifluoromethyl)phenyl]-1H-imidazole (3ci): 450.4 mg, 84% yield; white powder, mp: 154–156 °C; IR (KBr): ν 3450, 2924, 1619, 1496, 1327, 1167, 1134, 1073, 832 cm^{-1} ; ^1H NMR (400 MHz, CDCl_3): δ 3.54 (s, 3H), 7.27 (d, $J = 8.0$ Hz, 2H), 7.36 (d, $J = 8.8$ Hz, 2H), 7.39 (d, $J = 8.8$ Hz,

2H), 7.64 (d, $J = 8.4$ Hz, 2H), 7.77 (d, $J = 8.0$ Hz, 2H), 7.88 (d, $J = 8.0$ Hz, 2H); ^{13}C NMR (100 MHz, CDCl_3): δ 33.4, 120.8, 122.6, 123.5, 125.3, 125.6 (q, $J_{\text{C-F}} = 3.0$ Hz), 128.5, 129.2, 130.1, 130.7, 131.1, 131.4, 132.3, 132.6, 132.8, 137.5, 146.8; HREI-MS (m/z) calcd. for $\text{C}_{23}\text{H}_{15}\text{N}_2\text{Br}_2\text{F}_3$ (M) 533.9554, found 533.9541, calcd. for $\text{C}_{23}\text{H}_{14}\text{N}_2\text{Br}_2\text{F}_3$ (M - H) 532.9476, found 532.9478.

4,5-Bis(4-bromophenyl)-1-methyl-2-(4-nitrophenyl)-1H-imidazole (3cj): 456.7 mg, 89% yield; yellow powder, mp: 131–133 °C; IR (KBr): ν 3433, 2920, 1637, 1522, 1344 cm^{-1} ; ^1H NMR (400 MHz, CDCl_3): δ 3.59 (s, 3H), 7.27 (d, $J = 8.0$ Hz, 2H), 7.38 (s, 4H), 7.66 (d, $J = 8.0$ Hz, 2H), 7.98 (d, $J = 8.4$ Hz, 2H), 8.36 (d, $J = 8.4$ Hz, 2H); ^{13}C NMR (100 MHz, CDCl_3): δ 33.6, 121.0, 123.7, 124.0, 128.5, 129.0, 129.4, 131.0, 131.5, 132.2, 132.7, 132.8, 136.6, 138.2, 146.0, 147.7. HREI-MS (m/z) calcd. for $\text{C}_{22}\text{H}_{15}\text{N}_3\text{O}_2\text{Br}_2$ (M) 510.9531, found 510.9534.

Cyclic Voltammetry Measurements. Cyclic voltammograms were measured using a 273A Potentiostat/Galvanostat (Princeton Applied Research) equipped with an electrochemical analysis software, using a conventional three-electrode cell. The working electrode was a glassy carbon disk electrode (ca. $\phi = 3$ mm). The auxiliary and reference electrodes for these studies corresponded to a Pt wire and Ag/AgCl (in 3 M KCl), respectively; LiClO_4 (0.2 mol L^{-1}) in a solution of acetonitrile and dichloromethane (4:1 by volume) was used as the supporting electrolyte system. The concentration of each triarylimidazole was 1 mmol L^{-1} .

Calculations. Calculations were performed using the Spartan '08 software package.¹² As indicated in the text, the quantities used to calculate IP values refer to energy minimized structures for both the neutral and cation radical forms, in acetonitrile as the solvent. The B3LYP hybrid functional was used along with the 6-31+G(d) basis set.

■ ASSOCIATED CONTENT

☎ Supporting Information

Crystallographic data (CIF) and thermal ellipsoid plot for structure **3ac**, a table of redox data for 30 imidazole mediators, CV curves for redox catalysts **3ag**, **3bc** and **3ch** and their quasi-reversible first oxidation peak, ^1H and ^{13}C NMR spectral data for imidazole redox catalysts. This material is available free of charge via the Internet at <http://pubs.acs.org>.

■ AUTHOR INFORMATION

Corresponding Author

*zengcc@bjut.edu.cn; little@chem.ucsb.edu

Notes

The authors declare no competing financial interest.

■ ACKNOWLEDGMENTS

This work was supported by Grants from the National Natural Science Foundation of China (No. 21272021), Beijing Natural Science Foundation (No. 7112008), the National Key Technology R&D Program (2011BAD23B01), the National Basic Research Program of China (No. 2009CB930200) and a fund to C.-C.Z. from the Beijing City Education Committee (KM201010005009). R.D.L., C.M.L. and R.K.G. thank Amgen and Clorox for donations in support of education, R.D.L. thanks the UCSB Academic Senate Council on Research and Instructional Resources, and R.K.G. and R.D.L. thank the National Science Foundation PIRE-ECCI Program for a fellowship to R.K.G. (NSF PIRE-ECCI Fellow). We are grateful to Dr. Guang Wu (UCSB) for the x-ray analysis of structure **3ac**, and Dr. James Pavlovich (UCSB) for performing the mass spectral analyses.

■ DEDICATION

We dedicate this manuscript to the memory of R.D.L.'s wonderful mentor and friend, Howard E. Zimmerman.

■ REFERENCES

- (1) (a) Turro, N. J.; Scaiano, J. C.; Ramamurthy, V. *Modern Molecular Photochemistry of Organic Molecules*; University Science Books: New York, 2010. (b) Bauld, N. L.; Bellville, D. J.; Harirchian, B.; Lorenz, K. T.; Pabon, R. A., Jr; Reynolds, D. W.; Wirth, D. D.; Chiou, H.-S.; Marsh, B. K. *Acc. Chem. Res.* **1987**, *20*, 371–378. (c) Lu, Z.; Yoon, T. P. *Angew. Chem., Int. Ed.* **2012**, *51*, 10329–10332 and references therein. (d) Ischay, M. A.; Yoon, T. P. *Eur. J. Org. Chem.* **2012**, 3359–3372.
- (2) (a) Fry, A. J. *Synthetic Organic Electrochemistry*, 2nd ed.; Wiley: New York, 1989; (b) Evans, D. H. *Chem. Rev.* **2008**, *108*, 2113–2144. (c) Little, R. D.; Moeller, K. D. *Electrochem. Soc. Interface* **2002**, *11*, 36–42.
- (3) Zeng, C.-C.; Zhang, N.-T.; Lam, C. M.; Little, R. D. *Org. Lett.* **2012**, *14*, 1314–1317.
- (4) (a) Steckhan, E. *Angew. Chem., Int. Ed.* **1986**, *25*, 683–70. (b) Shirota, Y.; Kageyama, H. *Chem. Rev.* **2007**, *107*, 953–1010. (c) Gretton, M. J.; Kamino, B. A.; Brook, M. A.; Bender, T. P. *Macromolecules* **2012**, *45*, 723–728.
- (5) (a) Thomas, B.; David, C.; Muller, M. G.; Klaus, M.; Oskar, N. *Macromol. Rapid Commun.* **2000**, *21*, 583–589. (b) Moerner, W. E.; Scott, M. S. *Chem. Rev.* **1994**, *94*, 127–155.
- (6) For a tabulation of σ^+ values, see: Gordon, A. J.; Ford, R. A. *The Chemist's Companion*; Wiley: New York, 1972; pp 145–153.
- (7) Karimi-Jaberi, Z.; Barekat, M. *Chin. Chem. Lett.* **2010**, *21*, 1183–1185.
- (8) Wu, X.; Davis, A. P.; Lambert, P. C.; Steffen, L. K.; Toy, O.; Fry, A. J. *Tetrahedron* **2009**, *65*, 2408–2414.
- (9) Strictly speaking, the calculated values do not correspond to ionization potentials (IP). By definition, IP refers to the gas phase and to a vertical excitation where the geometry does not change. In contrast, the values we have calculated are based upon geometry-optimized structures and solvent-corrected energies. We have chosen this approach because of the vastly different time scales associated with a vertical excitation and a voltammetric measurement.
- (10) The correlation of redox potential with substituent constants is, of course, not new; an excellent discussion is found in: Zuman, P. *Substituent Effects in Organic Polarography*; Plenum Press: New York, 1967.
- (11) Davis, A. P.; Fry, A. J. *J. Phys. Chem. A* **2010**, *114*, 12299–12304.
- (12) Calculations were performed using the Spartan '08 software package. For detail, see: Shao, Y.; Molnar, L. F.; Jung, Y.; Kussmann, J.; Ochsenfeld, C.; Brown, S. T.; Gilbert, A. T. B.; Slipchenko, L. V.; Levchenko, S. V.; O'Neill, D. P.; DiStasio, R. A., Jr.; Lochan, R. C.; Wang, T.; Beran, G. J. O.; Besley, N. A.; Herbert, J. M.; Lin, C. Y.; Van Voorhis, T.; Chien, S. H.; Sodt, A.; Steele, R. P.; Rassolov, V. A.; Maslen, P. E.; Korambath, P. P.; Adamson, R. D.; Austin, B.; Baker, J.; Byrd, E. F. C.; Dachsel, H.; Doerksen, R. J.; Dreuw, A.; Dunietz, B. D.; Dutoi, A. D.; Furlani, T. R.; Gwaltney, S. R.; Heyden, A.; Hirata, S.; Hsu, C.-P.; Kedziora, G.; Khalliulin, R. Z.; Klunzinger, P.; Lee, A. M.; Lee, M. S.; Liang, W. Z.; Lotan, I.; Nair, N.; Peters, B.; Proynov, E. I.; Pieniazek, P. A.; Rhee, Y. M.; Ritchie, J.; Rosta, E.; Sherrill, C. D.; Simmonett, A. C.; Subotnik, J. E.; Woodcock, H. L., III; Zhang, W.; Bell, A. T.; Chakraborty, A. K.; Chipman, D. M.; Keil, F. J.; Warshel, A.; Hehre, W. J.; Schaefer, H. F.; Kong, J.; Krylov, A. I.; Gill, P. M. W.; Head-Gordon, M. *Phys. Chem. Chem. Phys.* **2006**, *8*, 3172–3191.
- (13) We are not claiming that our rule of thumb constitutes an original contribution. Our intent is simply to draw attention to one of the very attractive features associated the use of mediators. We are well aware of the pioneering contributions of Steckhan; see reference 4a for example, as well as: Steckhan, E. *Organic syntheses with electrochemically regenerable redox systems*. In *Topics in Current Chemistry, Electrochemistry I*; Steckhan, E., Ed.; Springer: Berlin, 1987; Vol. 142. There, he wrote: "It is very exciting that not only overpotentials can be eliminated but frequently redox catalysts can be applied with potentials which are 600 mV or in some cases even up to 1 Volt lower than the electrode potentials of the substrates." Given this comment, the reader will recognize that our "500 mV rule of thumb" is conservative, and deliberately so.
- (14) (a) Miranda, J.; Wade, C.; Little, R. D. *J. Org. Chem.* **2005**, *70*, 8017–8026. (b) Park, Y. S.; Little, R. D. *J. Org. Chem.* **2008**, *73*, 6807–6815. (c) Simonet, J.; Pilard, J.-F. *Electrogenerated Reagents*. In *Organic Electrochemistry*, 4th ed.; Lund, H., Hammerich, O., Eds.; Dekker: New York, 2001; Chapter 29.
- (15) We suspect, but have not proven, that the in situ formation of structures like **6**, generated via an intramolecular Friedel–Crafts-like cyclization of the initially formed cation radical may be responsible for the fact that in some cases, the first redox couple is quasi- rather than fully reversible.
- (16) Sanaeva, E. P.; Tanaseichuk, B. S. Deposited Doc. 1981, SPSTL 426 Khp-D81.
- (17) Alireza, E.; Abdolkarim, Z.; Mohsen, S.; Javad, A. R. *J. Comb. Chem.* **2010**, *12*, 844–849.
- (18) Srinivas, K.; Srinivas, U.; Bhanuprakash, K.; Harakishore, K.; Murthy, U. S. N.; Rao, V. J. *Eur. J. Med. Chem.* **2006**, *41*, 1240–1246.
- (19) Santos, J.; Mintz, E. A.; Zehnder, O.; Bosshard, C.; Bu, X. R.; Gunter, P. *Tetrahedron Lett.* **2001**, *42*, 805–808.